

AperTO - Archivio Istituzionale Open Access dell'Università di Torino

Nitric oxide and P-glycoprotein modulate the phagocytosis of colon cancer cells

This is the author's manuscript

Original Citation:

Availability:

This version is available <http://hdl.handle.net/2318/130251> since

Published version:

DOI:10.1111/j.1582-4934.2010.01137.x

Terms of use:

Open Access

Anyone can freely access the full text of works made available as "Open Access". Works made available under a Creative Commons license can be used according to the terms and conditions of said license. Use of all other works requires consent of the right holder (author or publisher) if not exempted from copyright protection by the applicable law.

(Article begins on next page)



UNIVERSITÀ DEGLI STUDI DI TORINO

This is an author version of the contribution published on:

[J Cell Mol Med.](#) 2011 Jul;15(7):1492-504. doi: 10.1111/j.1582-4934.2010.01137.x.

The definitive version is available at:

<http://onlinelibrary.wiley.com/doi/10.1111/j.1582-4934.2010.01137.x/abstract;jsessionid=B506B22DADC4C80684F4EA892DBAB10E.f03t01>

Nitric oxide and P-glycoprotein modulate the phagocytosis of colon cancer cells.

Joanna Kopecka^{1,§}, Ivana Campia^{1, §}, Davide Brusa², Sophie Doublier^{1,3}, Lina Matera^{2,3}, Dario Ghigo^{1,3}, Amalia Bosia^{1,3}, Chiara Riganti^{1,3,*}

¹ Department of Genetics, Biology and Biochemistry, University of Turin, via Santena 5/bis, 10126 Turin, Italy

² Department of Internal Medicine, Laboratory of Tumour Immunology, University of Turin, corso Dogliotti 14, 10126 Turin, Italy

³ Research Center on Experimental Medicine (Ce.R.M.S.), University of Turin, via Santena 5/bis, 10126 Turin, Italy

[§] These authors contributed equally to this work.

* Corresponding author: Dr. Chiara Riganti, Department of Genetics, Biology and Biochemistry, University of Turin, via Santena 5/bis, 10126 Turin, Italy; tel: +390116705851; fax: +390116705845; email: chiara.riganti@unito.it

Abstract

The anticancer drug doxorubicin induces the synthesis of nitric oxide (NO), a small molecule that enhances the drug cytotoxicity and reduces the drug efflux through the membrane pump P-glycoprotein (Pgp). Doxorubicin also induces the translocation on the plasma membrane of the protein calreticulin (CRT), which allows tumour cells to be phagocytized by dendritic cells. We have shown that doxorubicin elicits NO synthesis and CRT exposure only in drug-sensitive cells, not in drug-resistant ones, which are indeed chemo-immunoresistant. In this work we investigate the mechanisms by which NO induces the translocation of CRT and the molecular basis of this chemo-immunoresistance. In the drug-sensitive colon cancer HT29 cells doxorubicin increased NO synthesis, CRT exposure and cells phagocytosis. NO promoted the translocation of CRT in a cGMP- and actin cytoskeleton-dependent way. CRT translocation did not occur in drug-resistant HT29-dx cells, where the doxorubicin-induced NO synthesis was absent. By increasing NO with stimuli other than doxorubicin, the CRT exposure was obtained also in HT29-dx cells. However, whereas in sensitive cells the CRT translocation was followed by the phagocytosis, in drug-resistant cells the phagocytosis did not occur despite the CRT exposure. In HT29-dx cells CRT was bound to Pgp and only by silencing the latter the CRT-operated phagocytosis was restored, suggesting that Pgp impairs the functional activity of CRT and the tumour cells phagocytosis. Our work suggests that the levels of NO and Pgp critically modulate the recognition of the tumour cells by dendritic cells, and proposes a new potential therapeutic approach against chemo-immunoresistant tumours.

Keywords: doxorubicin, nitric oxide, P-glycoprotein, drug resistance, calreticulin, phagocytosis, dendritic cells, colon cancer

Introduction

The anthracycline doxorubicin has the peculiarity of inducing the synthesis of nitric oxide (NO), a small signalling molecule which plays an important role in cell growth, differentiation and apoptosis [1]. The effect of doxorubicin is mediated by the drug-induced activation of the transcriptional factor NF- κ B, which in turn up-regulates the transcription of the inducible NO synthase (*iNOS*; EC 1.14.13.39) gene, leading to the production of huge amounts of NO [2]. It has been suggested that at least part of the cytotoxic effects elicited by doxorubicin are due to the increased NO synthesis [3, 4]. NO also reduces the rate of doxorubicin efflux through ATP-binding cassette (ABC) membrane pumps, such as P-glycoprotein (Pgp) and multidrug resistance related protein 3 (MRP3), two transporters that are responsible for the resistance towards doxorubicin in cancer cells [5]. By nitrating these proteins on tyrosine residues, NO reduces Pgp and MRP3 activity, reversing doxorubicin-resistance in solid tumours [4, 6]. Notably, in doxorubicin-resistant cells the induction of *iNOS* gene is absent, in consequence of the fast drug extrusion; however when the NO levels are increased in resistant cells by agents other than doxorubicin, the drug efflux is reduced and the cytotoxicity is restored [4].

A great interest has been raised by the discovery that, besides exerting a direct anticancer effect, anthracyclines also stimulate the host immune response against the tumour [7, 8]. It has been discovered that the anthracyclines immunogenicity relies on their ability to induce the tumour cells phagocytosis by immature dendritic cells (iDCs). After this step, iDCs are stimulated to further mature and to raise a complete immune response against transformed cells [8]. Following doxorubicin exposure, a change in tumour cell plasma membrane occurs, leading to the exposure of intracellular proteins, such as calreticulin (CRT), which is recognized by iDCs and triggers the iDCs-mediated phagocytosis [8, 9]. CRT is usually

present in the endoplasmic reticulum (ER), where it acts as a chaperon and a Ca^{2+} sensor protein [8, 10].

We have recently demonstrated that doxorubicin mediates the exposure of CRT and the phagocytosis by iDCs thanks to the induction of iNOS in drug-sensitive cells: indeed neither the translocation of CRT nor the phagocytosis occurred in the doxorubicin-sensitive cells silenced for *iNOS* gene. Doxorubicin was devoid of pro-immunogenic effects also in drug-resistant cells, where the anthracycline was not able to accumulate at a sufficient extent to increase the synthesis of NO [6]. These results suggested that chemo- and immunoresistance to doxorubicin are strictly associated, and may both depend on the lack of NO synthesis in drug-resistant cells.

In the present work we first investigated the molecular mechanisms by which high levels of NO induce the translocation of calreticulin to the cell surface, comparing the doxorubicin-sensitive human colon cancer HT29 cells and the doxorubicin-resistant HT29-dx cells.

Moreover we observed that NO was sufficient to promote the translocation of CRT followed by the phagocytosis in drug-sensitive cells and was necessary to elicit the CRT exposure also in drug-resistant cells, but surprisingly the drug-resistant cells remained poorly phagocitized even in the presence of CRT levels superimposable to sensitive cells. We thus focused on the molecular basis of this strong association between chemo- and immunoresistance, and we analyzed if the increased expression of Pgp in drug-resistant cells may affect the CRT-mediated phagocytosis, thus contributing to their immunoresistant phenotype.

Materials and methods

Materials.

Foetal bovine serum (FBS), penicillin-streptomycin (PS) and RPMI 1640 were supplied by Sigma Chemical Co (St. Louis, MO), plasticware for cell culture was from Falcon (BD

Biosciences, Bedford, MA). Electrophoresis reagents were obtained from Bio-Rad Laboratories (Hercules, CA), the protein content of cell monolayers and cell lysates was assessed with the bicinchoninic acid kit from Sigma Chemical Co. Recombinant human tumour necrosis factor- α (TNF- α) was obtained from R&D Systems (Minneapolis, MN), 8-bromoguanosine-3':5'-cyclic monophosphorothioate, Rp-isomer (Rp-8-Br-cGMPS) from Calbiochem (San Diego, CA), latrunculin A was from Enzo Life Sciences International Inc (Plymouth Meeting, PA). When not otherwise specified, all the other reagents were purchased from Sigma Chemical Co.

Cells.

Human colon cancer cells (HT29 cell line, provided by Istituto Zooprofilattico Sperimentale "Bruno Umbertini", Brescia, Italy) were cultured in RPMI 1640 medium supplemented with 10% FBS, 1% PS and 1% L-glutamine, and maintained in a humidified atmosphere at 37°C and 5% CO₂. A subpopulation of HT29 cells, named HT29-dx, characterized by resistance to doxorubicin, was generated as previously described [4]. In the present study the drug resistance was previously assessed by measuring the Pgp/MRP3 expression, the intracellular doxorubicin accumulation and the drug-induced cytotoxicity, by FACS analysis of cells positive for annexin V-fluorescein isothiocyanate (FITC) as described [2] (data not shown).

Nitrite production.

Then nitrite production was measured by adding 0.15 mL of cell culture medium to 0.15 mL of Griess reagent in a 96-well plate, and after a 10 min incubation at 37° in the dark, the absorbance was measured at 540 nm with a Packard EL340 microplate reader (Bio-Tek Instruments, Winooski, VT). A blank was prepared for each experimental condition in the absence of cells, and its absorbance was subtracted from the one obtained in the presence of cells. Nitrite concentration was expressed as nanomoles of nitrite/mg cell proteins.

Measurement of NOS Activity.

The procedure described in Ghigo et al. [11] was followed. The cells were detached with 0.05% v/v trypsin, washed with PBS, re-suspended at the concentration of 100 µg cell proteins in 0.6 mL of 20 mmol/L Hepes buffer (pH 7.2) and sonicated with one 10 s burst, using a Labsonic Sonicator (Hielscher, Teltow, Germany). 15 µL of lysate was withdrawn to assess the protein content. The protease inhibitors pepstatin (75 µmol/L) and leupeptin (20 µmol/L) were added to the cell lysate, which was then mixed with the following reagents in a 500 µL final volume: 0.2 mmol/L NADP⁺, 360 µmol/L L-arginine, 2 µmol/L tetrahydrobiopterin, 0.3 mmol/L CaCl₂, 0.2 mmol/L dithiothreitol, 1.8 mmol/L MgCl₂, 0.17 mmol/L glucose 6-phosphate, and 40 mU/mL glucose 6-phosphate dehydrogenase (G6PD; from *Saccharomyces cerevisiae*; EC 1.1.1.49). The NOS/G6PD reaction mixture was incubated at 37°C for 3 h, then heated at 100°C for 5 min to inactivate G6PD. To oxidize the remaining NADPH, which might interfere with the subsequent Griess reaction, the mixture was incubated with 10 mU/mL L-lactate dehydrogenase (from pig muscle; EC 1.1.1.27) and 300 µmol/L sodium pyruvate at 37°C for 5 min. The nitrite production was measured using the Griess reagent as described. Blanks were prepared by replacing the cell lysate with Hepes solution, in the NOS/G6PD reaction mix, which was subjected to the same experimental procedure used for samples containing lysate. The NOS activity was expressed as nanomoles nitrites/min/mg protein.

Analysis of cell surface CRT.

For flow cytometry analysis, cells were washed twice with PBS, rinsed with 1 mL of 0.25% w/v PBS-bovine serum albumin (BSA) and centrifuged at 10,000 x g for 5 min. The pelleted cells were incubated for 45 min (4°C) with an anti-CRT rabbit polyclonal antibody (Affinity Bioreagents, Rockford, IL), diluted 1:500 in 100 µL of PBS-BSA, then washed and incubated with 100 µL anti-rabbit FITC-conjugated antibody (diluted 1:50 in PBS-BSA) for 30 min at

4°C in the dark. After fixation in paraformaldehyde 2%, cells were re-suspended in 500 µL PBS-BSA and analyzed using a FACS-Calibur system (BD Biosciences). For each analysis 10,000 events were collected. The percentage of fluorescent cells was calculated by the Cell Quest software (BD Biosciences). Control experiments included incubation of cells with non-immune isotypic antibodies followed by the appropriate labelled secondary antibody. Since doxorubicin has a strong autofluorescence which might lead to misinterpret flow cytometry results, we validated FACS experiments by measuring the calreticulin exposure in biotinylation assays, using the Cell Surface Protein isolation kit from Thermo Fisher Scientific Inc. (Rockford, IL), as previously reported [6]. 25 µg of the biotinylated proteins were separated by 10% SDS-PAGE, transferred to a PVDF membrane sheet (Immobilon-P, Millipore, Billerica, MA) and probed with the anti-CRT rabbit polyclonal antibody (diluted 1:1,000 in PBS-BSA 1%). The whole cellular content of CRT was measured after ultracentrifugation of the cell lysates at 100,000 x g for 1 h. 10 µg of the pelleted proteins were separated by 10 % SDS-PAGE, transferred to PVDF membrane sheet and probed with the anti-CRT antibody. The membranes were washed with PBS-Tween 0.1% and subjected for 1 h to a horseradish peroxidase-conjugated anti-rabbit antibody (diluted 1:3000 in PBS-Tween 0.1% with blocker non fat dry milk 5%, Bio-Rad). The membranes were washed again and the proteins were detected by enhanced chemiluminescence (PerkinElmer, Waltham, MA).

In vitro phagocytosis assay.

Immature dendritic cells (iDC) were generated as described [12]. The tumour cells were green-stained with PKH2-FITC (Sigma Chemical Co.), washed twice and incubated for 20 h at 37°C with 1×10^5 iDC at a 1:1 ratio, and the mixed culture was stained with the phycoerythrin (PE)-conjugated anti-CD80 antibody (BD Bioscience) for 20 min at 4°C. Phagocytosis of tumour cells by iDC was assessed by flow cytometric analysis as the percentage of double-stained (FITC plus PE) versus red (PE) stained cells on a total of 10,000

events, using the DIVA software (FacsCanto system, BD). A phagocytosis assay was performed by co-incubating iDC and tumour cells at 4°C, instead of 37°C, and the percentage of double-stained cells obtained after the incubation at 4°C was subtracted from the one obtained after a 37°C incubation. The phagocytosis rate was expressed as phagocytic index, calculated as previously reported [9].

Immunofluorescence microscopy.

Cells were seeded on sterile glass coverslips and incubated under the experimental conditions indicated in Results, then rinsed with PBS and fixed with 4% w/v paraformaldehyde for 15 min. To visualize intracellular CRT, the samples were permeabilized with 0.1% v/v Triton-X100 for 5 min on ice. Both permeabilized and non-permeabilized cells (used to detect surface CRT) were washed three times with PBS and stained with a rabbit polyclonal anti-CRT antibody (diluted 1:100 in PBS containing 1% FBS) for 1 h at room temperature. After washing, the samples were incubated with a biotinylated goat anti-rabbit IgG antibody (diluted 1:50; Vector Laboratories, Burlingame, CA) for 30 min at room temperature, washed and incubated with fluorescein avidin D (diluted 1:300, Vector Laboratories) for further 30 min at room temperature. To visualize actin cytoskeleton, cells were co-incubated with phalloidin-tetramethylrhodamine B isothiocyanate (diluted 1:1000). Finally all samples were washed with PBS, stained with 4',6-Diamidino-2-phenylindole dihydrochloride (DAPI; diluted 1:20,000) and washed again. The coverslips were mounted with 4 µl of Gel Mount Aqueous Mounting and examined with a Leica DC100 fluorescence microscope (Leica Microsystems GmbH, Wetzlar, Germany). For each experimental point, a minimum of 5 microscopic fields were examined.

Western blot analysis.

Cells were washed twice with PBS, then lysed in heated lysis buffer (25 mmol/L Hepes, 135 mmol/L NaCl, 1% v/v Nonidet P-40, 5 mmol/L EDTA, 1 mmol/L EGTA, 1 mmol/L ZnCl₂

and 10% v/v glycerol) and sonicated with one 10-s burst, using a Labsonic Sonicator (Hielscher, Teltow, Germany). After centrifugation (13,000 x g for 15 min) the protease inhibitor cocktail III (100 mmol/L AEBSF, 80 µmol/L aprotinin, 5 mmol/L bestatin, 1.5 mmol/L E-64, 2 mmol/L leupeptin, and 1 mmol/L pepstatin; Calbiochem), 2 mmol/L phenylmethylsulfonyl fluoride and 1 mmol/L NaVO₄ were added to the supernatant. 25 µg cell proteins were separated by SDS-PAGE, transferred to PVDF membrane sheets and probed with an anti-vasodilator-stimulated phosphoprotein (VASP) (rabbit polyclonal, diluted 1:500 in PBS-BSA 1%; Cell Signaling Technology Inc., Danvers, MA) or an anti-phospho(Ser 239)-VASP (mouse monoclonal, diluted 1:500 in PBS- non fat dry milk 3%, Millipore) antibody.

In co-immunoprecipitation experiments, 100 µg of total cell proteins or biotinylated proteins, re-suspended in 200 µL TEEN-Triton buffer (Tris 50 mmol/L, EDTA 1 mmol/L, EGTA 1 mmol/L, NaCl 150 mmol/L, Triton X-100 1% v/v), were immunoprecipitated overnight with the anti-CRT antibody (diluted 1:100), then subjected to 7% SDS-PAGE and probed for Pgp (with a rabbit polyclonal antibody, diluted 1:250 in PBS- non fat dry milk 5%, Santa Cruz Biotechnology Inc., Santa Cruz, CA). The proteins were detected by enhanced chemiluminescence as described above. The densitometric analysis of Western blots was performed using the ImageJ software (<http://rsb.info.nih.gov/ij/>) and expressed as arbitrary units, where “1 unit” is the mean band density of the experimental condition "HT29 CTRL".

Small interfering RNA (siRNA).

200,000 cells were plated and cultured in RPMI 1640 containing 10% FBS. After 24 h, cells were washed with 2 mL siRNA transfection medium (Santa Cruz Biotechnology Inc.) and incubated for 6 h with 1 mL siRNA transfection medium containing 5 µL of siRNA transfection reagent (Santa Cruz Biotechnology Inc.) and 50 pmol of Pgp specific siRNA (Santa Cruz Biotechnology Inc.). In each set of experiments, one dish was treated with 50

pmol of Control siRNA-A (Santa Cruz Biotechnology Inc.), a scrambled non targeting 20-to 25-nucleotide siRNA, designed as a negative control to assess siRNA specificity. At the end of the incubation, 1 mL of RPMI 1640 containing 1% PS and 20% FBS was added for 24 h; cells were washed and cultured for 72 h in RPMI 1640 with 1% PS and 10% FBS. To verify the siRNA efficacy, the expression of Pgp protein were analyzed by Western blotting as reported above. The expression of glyceraldehyde 3-phosphate dehydrogenase (GAPDH), chosen as a housekeeping gene, was checked with a specific antibody (from rabbit, diluted 1:500 in PBS-BSA 1%, Santa Cruz Biotechnology Inc.).

Intracellular doxorubicin accumulation.

Cells were grown in 35 mm-diameter Petri dishes and incubated in RPMI 1640 for 3 h with 5 μ mol/L doxorubicin, then the intracellular content of the drug was detected fluorimetrically as previously reported [4].

Statistical analysis.

All data in text and figures are provided as mean \pm SE. The results were analyzed by a one-way analysis of variance (ANOVA) and Tukey's test. $P < 0.05$ was considered significant.

Results

Doxorubicin fails to increase calreticulin exposure and HT29 cells phagocytosis when NO synthesis is inhibited.

Doxorubicin increased the activity of NOS enzyme (Figure 1A) and the synthesis of nitrite (Figure 1B) in HT29 cells; both the events were reversed by the NOS inhibitor N^G-monomethyl-L-arginine (L-NMMA). The NO scavenger 2-phenyl-4,4,5,5-tetramethylimidazoline-1-oxyl-3-oxide (PTIO), which *per se* did not affect the enzymatic activity of NOS (Figure 1A), effectively reduced the increase of nitrite elicited by the anthracycline (Figure 1B). By labelling the surface proteins of HT29 cells with biotin (Fig

1C) and by employing flow cytometry (Fig 1D), we showed that doxorubicin increased the amount of plasma membrane-associated CRT in HT29 cells and that this response was lowered by PTIO and L-NMMA. No change in total CRT was detected in the presence of doxorubicin, PTIO and L-NMMA (Figure 1C). Doxorubicin also enhanced the phagocytosis of HT29 cells by iDCs, but when the NO scavenger or the NOS inhibitor were co-incubated with the drug, the phagocytosis was lowered (Figure 1E).

On the opposite, doxorubicin, which was less accumulated in HT29-dx cells [6], did not elicit any increase of NO synthesis (Figure 1A and 1B), CRT translocation on plasma membrane (Figure 1C and 1D) and phagocytosis (Figure 1E) in drug-resistant cells. PTIO and L-NMMA were devoid of effects on all these parameters in HT29-dx cells (Figure 1A-E). HT29-dx cells exhibited a basally lower activity of NOS enzyme (Figure 1A), a result already reported in this experimental model [6]. Unexpectedly, we observed that the rate of phagocytosis in untreated HT29-dx cells was lower than in HT29 cells (Figure 1E).

NO promotes the translocation of calreticulin in a cGMP-dependent way, via the actin cytoskeleton remodelling.

Amongst its several target enzymes, NO may activate a soluble guanylate cyclase (sGC) and increase the synthesis of cGMP, which in turn promotes the activation of a cGMP-dependent protein kinase (PKG). This event accounts for several effects of NO such as smooth muscle relaxation, platelet aggregation and cytoskeleton remodelling [13]. Therefore we measured the expression of cell surface CRT in the presence of the NO donor S-nitrosopenicillamine (SNAP), of the stable cGMP analogue 8-Br-cGMP, of the sGC inhibitor 1H-

[1,2,4]oxadiazolo-[4,3-a]quinoxalin-1-one (ODQ) and of the PKG inhibitor Rp-8-Br-cGMPS. 8-Br-cGMP was as effective as SNAP in inducing the translocation of CRT (Figure 2A and 2B). On the contrary, ODQ and Rp-8-Br-cGMPS greatly reduced the effect of SNAP (Figure

2A and 2B). Remarkably, the response to cGMP pathway modulators was similar in doxorubicin-sensitive and doxorubicin-resistant cells.

Immunofluorescence analysis revealed that untreated HT29 and HT29-dx cells had no detectable amounts of CRT on plasma membrane, whereas the great majority of the protein was contained within cells (Figure S1). NO promoted the translocation of CRT in a time-dependent way: indeed CRT was nearly undetectable 10 min after the application of SNAP, but became more appreciable after 30 minutes. At 1 h the fluorescence was more intense and detected on larger portions of cell surface. Again, the response to the NO donor was superimposable in chemo-sensitive and chemo-resistant cells (Figure S1), as observed in flow cytometry analysis (Figure 2A) and biotinylation assay (Figure 2B).

A downstream effector of PKG is the vasodilator-stimulated phosphoprotein (VASP), which, after being phosphorylated on serine by PKG, has a prominent role in actin cytoskeleton remodelling [14]: in HT29 and HT29-dx cells the phosphorylation of VASP was absent under basal conditions, became detectable in the presence of SNAP and 8-Br-cGMP, and was reduced to zero when SNAP was co-incubated with ODQ and Rp-8-Br-cGMPS (Figure 2C). Total VASP did not vary in any experimental condition (Figure 2C).

To evaluate the involvement of actin cytoskeleton in the NO/cGMP-mediated translocation of CRT, we analyzed the effect of latrunculin A, a specific inhibitor of G-actin monomers assembly: interestingly, SNAP and 8-Br-cGMP were not able to elicit any detectable exposure of CRT in both HT29 and HT29-dx cells, when co-incubated with latrunculin A (Figure 3A and 3B). Untreated HT29 and HT29-dx cells showed a widespread intracellular actin distribution, with a continuous ring in the sub-plasma membrane region (Figure 3C). Such a distribution was not modified by the SNAP, whereas latrunculin, both alone and in the presence of the NO donor, induced a pronounced change in cell morphology, disrupted the sub-plasma membrane ring and condensed actin in selective areas of cells surface. Moreover

when co-incubated with latrunculin, SNAP was not able to elicit the translocation of CRT on cell plasma membrane (Figure 3C).

Taken together these results indicate that NO elicits the translocation of CRT on plasma membrane, via the cGMP/PKG/VASP activation and the remodelling of actin cytoskeleton. This pathway is as active in chemosensitive as in chemoresistant cells.

CRT exposure is increased by NO in both HT29 and HT29-dx cells, but is followed by phagocytosis only in doxorubicin-sensitive cells.

TNF- α , a potent inducer of iNOS, significantly increased the NOS activity (Figure 4A), the nitrite levels (Figure 4B) and the CRT translocation (Figure 4C and 4D) in both doxorubicin-sensitive and doxorubicin-resistant cells. PTIO, which lowered the levels of nitrite (Figure 4B) without affecting *per se* NOS activity (Figure 4A), also decreased the exposure of CRT (Figure 4C and D). In parallel TNF- α induced, whereas PTIO reduced, the index of phagocytosis of HT29 cells by iDCs (Figure 4E). Despite the increase of nitrite and CRT, TNF- α did not induce the iDCs-mediated uptake of HT29-dx cells, which were less phagocytized than drug-sensitive cells in each experimental condition (Figure 4E).

Doxorubicin and the NO donor SNAP *per se* increased the nitrite levels (Figure 5A) and the CRT exposure (Figure 5C and 5D) in HT29 cells, displaying an additive effect when co-incubated (Figure 5A, 5C and D). SNAP did not modify the activity of NOS, which was raised by doxorubicin in sensitive cells and remained superimposable to the control cells in all the other conditions (Figure 5B), but increased the nitrite amounts by releasing NO (Figure 5A). When SNAP was co-incubated with doxorubicin in doxorubicin-resistant cells, where the drug alone was devoid of effect, the nitrite amount was significantly increased (Figure 5A) and the CRT exposure was induced (Figure 5C and D). Cisplatin, an anticancer agent which did not affect the NO synthesis (Figure 5A and 5B) was not able to elicit any

translocation of CRT (Figure 5C and 5D) or to promote the phagocytosis (Figure 5E). However, when SNAP was added to cisplatin, the CRT expression became detectable in plasma membrane (Figure 5C and 5D) and the uptake of HT29 cells by iDCs was significantly raised (Figure E). Again, a dissociation between the CRT exposure and the phagocytosis was observed in HT29-dx cells, where in the presence of cisplatin plus SNAP, the CRT translocation on cell surface increased (Fig 5C and 5D), but the phagocytosis did not (Fig 5E).

These data gave us further evidences that NO, generated by an iNOS inducer as well as released by a NO donor, was necessary to promote the CRT translocation in both doxorubicin-sensitive and -resistant tumour cells, but it was sufficient to induce phagocytosis by iDCs only in the drug-sensitive ones.

In HT29-dx cells calreticulin is associated to Pgp, which exerts an inhibitory effect on the phagocytosis.

To analyze why the increased amount of surface CRT was not relatable to an increased phagocytosis in HT29-dx cells, we investigated whether P-glycoprotein, a membrane protein which is overexpressed in HT29-dx cells, but not in HT29 cells [4, 6], might interfere with the functional activity of the surface CRT or with the phagocytosis of drug-resistant cells. We first assessed if Pgp was physically associated to CRT: we immunoprecipitated with an anti-CRT antibody the cell extracts enriched with the ER membranes (where the vast majority of CRT resides) or containing the cell surface biotinylated proteins; then we probed the immunoprecipitated samples with an anti-Pgp antibody (Figure 6). In HT29 cells, where the expression of Pgp was low (Figure 7A), we did not detect any association between Pgp and CRT (Figure 6A). On the opposite, in ER extracts derived from HT29-dx cells, Pgp co-immunoprecipitated with CRT (Figure 6A). Such an association was detected in untreated cells and was not affected by doxorubicin or SNAP (Figure 6A). The NO donor SNAP was

the only agent able to induce the exposure of CRT in the plasma membrane in HT29-dx cells (Figure 5B, 5C and 6B): following SNAP incubation, we observed a co-immunoprecipitation of CRT and Pgp also in the cell extracts containing surface biotinylated proteins (Figure 6B). This phenomenon was absent in untreated cells and in HT29-dx cells exposed to doxorubicin (Figure 6B). Such a result suggests that Pgp was bound to CRT in ER and that this association was not lost during the translocation on the plasma membrane of doxorubicin-resistant cells. To further clarify whether the interaction between CRT and Pgp has a functional role in the immuno-resistance of HT29-dx cells, we knocked down Pgp with a siRNA approach. Besides reducing the protein expression levels in HT29-dx cells (Figure 7A), the silencing of Pgp raised the accumulation of doxorubicin to a level superimposable to that of not-silenced HT29-dx cells treated with SNAP (Figure 7B). Wild type HT29-dx and HT29-dx Pgp⁻ cells did not differ in nitrite levels (Figure 7B) and surface CRT amounts (Figure 7C) under basal conditions and after the incubation with SNAP. On the contrary, doxorubicin was able to increase the NO synthesis (Figure 7B) and the CRT exposure on the plasma membrane (Figure 7C) only in HT29-dx cells silenced for Pgp, where the drug intracellular content was significantly higher (Figure 7B). As far as the uptake by iDCs is concerned, untreated HT29-dx Pgp⁻, which exhibited a low exposure of CRT (Figure 7C), were poorly phagocytized, similarly to HT29-dx cells (Figure 7D). However, in the presence of doxorubicin or SNAP, which both increased the surface CRT levels in HT29-dx Pgp⁻ cells (Figure 7C), the silencing of Pgp induced the uptake by iDCs, suggesting that the overexpression of Pgp exerts a negative control on the CRT-dependent phagocytosis of drug-resistant cells (Figure 7D).

Discussion

The combination of conventional anticancer drugs to immunostimulating agents has recently obtained promising results in tumour mice models and in clinical trials [15, 16].

Anthracyclines, like doxorubicin, are useful tools in the chemoimmunotherapy, because they are the only anticancer drugs with a proved stimulating effect on macrophages [17], lymphocytes [18] and DCs [8]. Most anticancer drugs elicit in tumour cells an apoptotic death, which is considered not immunogenic, in opposition to a necrotic death, which releases in the microenvironment several tumour antigens, recognized by iDCs [8]. Doxorubicin exerts both an apoptotic and an immunogenic cell death: indeed following the drug administration, several intracellular proteins, like CRT, are exposed on the plasma membrane and trigger the tumour cells uptake by iDCs [8]. Besides inducing CRT translocation, doxorubicin is also able to increase the synthesis of NO, which may act as a tumoricidal agent, as an immunomodulator agent [19] and as an inhibitor of the doxorubicin efflux through ABC-transporters [4, 6]. We have recently demonstrated that NO is also the mediator of the CRT translocation in the HT29 doxorubicin-sensitive colon cancer cells: after this event, tumour cells are phagocytized by iDCs, which acquired the competence to prime alloantigen reactive lymphocytes [6]. No translocation of CRT is elicited by doxorubicin when the synthesis of NO is lacking, like in HT29 cells silenced for *iNOS* gene, or in doxorubicin-resistant HT29-dx cells, where the drug is actively extruded by Pgp and is not accumulated at a sufficient amount to raise the NO synthesis [6].

In the present work we first investigated by which mechanisms NO could exert such an effect. In chemosensitive HT29 cells incubated with doxorubicin, in the presence of a NO scavenger or a NOS inhibitor, the nitrite increase elicited by the anthracycline, the CRT translocation and the cells phagocytosis by iDCs were all reduced. On the contrary, in drug-resistant HT29-dx cells, where NO levels were not modulated by doxorubicin, PTIO and NMMA, CRT translocation and phagocytosis by iDCs remained low. Interestingly, NOS activity was lower in untreated HT29-dx cells than in HT29 cells, although no significant difference was detected in the nitrite levels between these cell populations: such a discrepancy is likely due

to the higher sensitivity of the spectrophotometric assay of NOS activity towards the colorimetric Griess method for nitrite detection [11]. We did not observe any variation in the total CRT expression, despite significant changes in the CRT levels on the plasma membrane. Most CRT usually resides in ER and is absent on plasma membrane, where only small amounts of CRT translocate; it has been suggested that, although the fraction of CRT in ER does not change, small variations in the plasma membrane fraction may be sensed as an effective “eat me” signal by iDCs [9]. The appearance of small but detectable amounts of CRT was a powerful eating marker also in our experimental model. This event has been reported to be the first step a more complex activation of the host immune system against the tumour.

For example the exposure of CRT on the mouse CT26 colon cells surface has been shown to trigger the activation of immune system cells in mice xenografts [9] and the up-regulation of CRT gene in colon cancers with microsatellite instability has been associated with a more pronounced lymphocytic infiltrate, a more active immune response and a better prognosis of patients [20]. In keeping with these observation, we have previously observed that in HT29 cells the CRT exposure increased the tumour cell uptake and the progression of immature DCs to an antigen-presenting mature phenotype [6].

Several mechanisms have been invoked to explain how CRT appears on the plasma membrane following anthracyclines administration. Since such a translocation occur in both enucleated and nucleated tumour cells, the increase of CRT on the cell surface is not attributable to augmented gene transcription [9]. Some experimental evidences show that agents preventing the ER stress, such as the inhibitors of PP1/GADD34 complex, facilitate the CRT translocation. However the inhibition of PP1/GADD34 *per se* is not sufficient to evoke an immunogenic death of tumour cells [9]. The human neuroblastoma SH-SY5Y cell line is completely refractory to translocate CRT in response to mitoxantrone, but the depletion

of Ca^{++} in ER partially restores this CRT translocation [21]. NO has already been reported to lower the Ca^{++} level in ER [22] and we cannot exclude that this mechanism could be implicated in the translocation of CRT from ER to the plasma membrane. However our results suggest an involvement of the cGMP/PKG pathway in such a translocation in colon cancer cells: indeed both the NO donor SNAP and the sGC activator 8-Br-cGMP increased CRT exposure, which was prevented by inhibiting sGC or PKG. When PKG is activated it can in turn phosphorylate and activate the serine-threonine kinase VASP [14], an event which was observed in both HT29 and HT29-dx cells stimulated by SNAP or 8-Br-cGMP and was reduced when the sGC/PKG pathway was blocked. Active VASP deeply affects the activity and localization of intercellular junction proteins and integrins, owing to its effect on actin cytoskeleton [13]. Interestingly, the anthracycline-mediated exposure of CRT in mouse colon cells was reduced by inhibiting the actin fibres remodelling, whereas was unaffected by agents disrupting microtubules [9]. In our experimental conditions, latrunculin A, a toxin inhibiting the polymerization of G-actin, blocked the CRT translocation elicited by SNAP or 8-Br-cGMP. Therefore we can hypothesize that NO promotes the exposure of CRT by activating the cGMP/PKG/VASP pathway and by inducing a remodelling of the actin fibres. NO promoted a time-dependent translocation on plasma membrane of CRT, which was concentrated in selective portions of cell surface. Such a patchy distribution was observed also in CT26 colon cancer cells exposed to mitoxanthrone, suggesting a preferential localization of CRT in specific microdomains of plasma membrane. In CT26 cells CRT co-localizes with ERp57, another protein of endoplasmic reticulum, which translocates on cell surface and becomes an integral component of the major histocompatibility complex class I system [23]. We cannot exclude that NO promotes a co-translocation of CRT and ERp57 from ER to plasma membrane also in HT29 colon cancer cells.

Notably no differences in the translocation of CRT induced by the NO/cGMP-pathway were detected between doxorubicin-sensitive and doxorubicin-resistant cells, suggesting that the downstream effectors of NO worked at the same extent in the two populations.

Similarly, if we increased the NO levels with a stimulus different from doxorubicin, such as the iNOS inducer TNF- α , the synthesis of nitrites and the translocation of CRT occurred in HT29 and in HT29-dx cells with no appreciable differences, suggesting that the lack of NO production in doxorubicin-treated HT29-dx was not due to a defect in the iNOS induction pathway, but rather to the inability to accumulate enough doxorubicin to activate the NF-kB signalling transduction.

Not all chemotherapeutic drugs exert pro-immunogenic effects; some non-immunogenic drugs, such as etoposide, camptothecine and mitomycin C, acquire pro-immunogenic properties only when co-administrated with recombinant CRT [9]. We show in the present work that the co-incubation with a NO donor may produce the same effect: indeed cisplatin did not increase NO levels and CRT exposure in HT29 and HT29-dx cells, but all these events were induced when cisplatin was associated to SNAP. Moreover when SNAP and doxorubicin were added together, they had a small but detectable additive effect on CRT translocation in HT29 cells, suggesting that 5 $\mu\text{mol/L}$ doxorubicin did not exert a maximal translocation and that NO may further increase the exposure of CRT elicited by doxorubicin in sensitive cells. On the other hand, when doxorubicin was devoid of effect, as it occurred in HT29-dx cells, the addition of SNAP restored the translocation of CRT.

Every time we detected an increase of CRT translocation in chemosensitive cells, we also observed an increased phagocytosis by iDCs. On the contrary, although the CRT density was as high on the HT29-dx cells surface as in HT29 cells (e.g. following TNF- α or SNAP), the phagocytosis of chemoresistant cells did not increase. Our results suggest that NO was sufficient to promote the CRT translocation followed by the phagocytosis in doxorubicin-

sensitive cells. The situation looks different in drug-resistant cells, where NO was necessary to induce the exposure of CRT, but this event was not sufficient to induce the uptake by iDCs. Interestingly also untreated HT29-dx cells were less phagocytized than HT29 cells: CRT was low in both the populations in this experimental condition, so we wondered if other additional features made doxorubicin-sensitive and doxorubicin-resistant cells different as to their phagocytosis by iDCs. A striking difference between HT29 and HT29-dx cells is the overexpression in the latter population of Pgp, which is responsible of the drug-resistant phenotype. We therefore evaluated whether this protein could play a role also in the immunoresistance of HT29-dx cells.

Surprisingly we found that CRT was bound to Pgp, in a manner dependent on the expression level of the latter. Indeed in HT29 cells Pgp was not co-immunoprecipitated with CRT, probably because of the very low amounts of this ABC-transporter. On the other hand, in HT29-dx cells, where the efflux pump is abundant, CRT clearly interacted with Pgp. Our results on the ER-enriched fraction and on the plasma membrane fraction suggest that such an association started in the ER membrane, where both calreticulin and Pgp are present [24], and was not lost during the movement to the cell surface. NO did not alter the binding of CRT with Pgp, since the interaction between them persisted in the presence of SNAP. It is conceivable that the activity of the NO/cGMP pathway is not specific for a single ER protein like CRT, but generically facilitates the traffic of microsomal vesicles from ER to plasma membrane. Acting as a chaperon protein, CRT may bind many other proteins synthesized in ER and help them in the intracellular processing and folding: for example it has been recently demonstrated that CRT forms complexes with collagen type I in the ER of fibroblasts. This association plays a crucial role in the trafficking of collagen from ER to Golgi apparatus and is important to target the collagen fibres to their final destination in the extracellular environment [25]. Since Pgp is actively synthesized in drug-resistant cells, we may suppose

that the ABC transporter interacts with CRT during the quality control step in the ER and that CRT acts as an escort protein for Pgp, accompanying the latter to its definitive localization on the plasma membrane. However, following this interaction, CRT loses at least one of its functional properties, that is the peculiarity to function as a docking protein for iDCs on tumour surface.

When the expression of Pgp was knocked down by specific siRNAs, the CRT-operated phagocytosis was restored in HT29-dx cells: in silenced cells doxorubicin was able again to accumulate, to induce NO synthesis and CRT translocation, and to promote phagocytosis by iDCs. Also SNAP, which was capable to induce the CRT exposure but not the phagocytosis in HT29-dx cells, became an “eat me” agent in Pgp-silenced HT29-dx cells, reproducing all the effects exhibited in drug-sensitive HT29 cells. These data show that Pgp, when overexpressed, inhibits the tumour cells phagocytosis and plays a role not only in the chemoresistance, but also in the immunoresistance. At the present we do not know the nature of the binding between CRT and Pgp, and the mechanism of the Pgp-mediated inhibition of phagocytosis. The ABC-transporter might exert a steric hindrance, due to its high molecular weight and abundance on cells surface of resistant cells, impairing the correct membrane presentation or clusterization of CRT and altering the recognition of tumour cells by iDCs. Chemo-immunotherapy is a very promising approach in the treatment of the most aggressive cancers, refractory to the conventional anticancer drugs [16]; a better knowledge of the mechanisms which regulate the chemo-immunoresistance to doxorubicin in human cancer cells is certainly useful to optimize the chemo-immunotherapeutic protocols. In our work we have demonstrated that the association of NO-releasing compounds, which are widely used in the management of cardiovascular diseases, to conventional anticancer drugs, may represent a novel approach of chemo-immunotherapy in chemosensitive tumours. As for the chemoresistant tumours, which we showed are also immunoresistant, NO was able to restore

the sensitivity to the doxorubicin cytotoxic effects and the translocation of CRT [4, 6], but was not sufficient to trigger the activation of iDCs against the tumour. However the refractoriness of drug-resistant cells to be phagocytized may be circumvented by down-regulating the Pgp protein. Recently the selective silencing of Pgp, followed by the administration of anticancer drugs, has successfully arrested the growth of chemoresistant tumour in mice xenografts, prolonging the overall survival of the animals and showing new possibilities of combination therapies for aggressive cancers [26]. Our work may suggest that the combination of NO-releasing agents with therapeutic tools down-regulating Pgp fully restores the functional role of CRT in drug-resistant cells and might be successful to obtain a reversion of chemo-and immunoresistance in these cells.

Acknowledgements

We are grateful to Mr. Costanzo Costamagna for the technical assistance provided and to Dr. Silvia Peola for the help with the flow cytometry analysis.

This work has been supported with grants from Fondazione Internazionale Ricerche Medicina Sperimentale (FIRMS), Compagnia di San Paolo, Regione Piemonte (Ricerca Sanitaria Finalizzata 2008 and 2009) and Ministero dell'Università e della Ricerca (Rome, Italy).

Conflict of interest disclosure.

The authors confirm that they have no conflicts of interests.

References

1. **Murphy MP.** Nitric oxide and cell death. *Biochim Biophys Acta* 1999; 1411: 401-14.

2. **Riganti C, Doublier S, Costamagna C, et al.** Activation of nuclear factor-kB pathway by simvastatin and RhoA silencing increases doxorubicin cytotoxicity in human colon cancer HT29 cells. *Mol Pharmacol.* 2008; 74: 476-84.
3. **Lind DS, Kontaridis MI, Edwards PD, et al.** Nitric oxide contributes to adriamycin's antitumor effect. *J Surg Res.* 1997; 69: 283-87.
4. **Riganti C, Miraglia E, Viarisio D, et al.** Nitric Oxide Reverts the Resistance to Doxorubicin in Human Colon Cancer Cells by Inhibiting the Drug Efflux. *Cancer Res.* 2005; 65: 516-25.
5. **Takara K, Sakaeda T, Okumura K.** An update on overcoming MDR1-mediated multidrug resistance in cancer chemotherapy. *Curr Pharm Des.* 2006; 12: 273-86.
6. **De Boo S, Kopecka J, Brusa D, et al.** iNOS activity is necessary for the cytotoxic and immunogenic effects of doxorubicin in human colon cancer cells. *Mol Cancer* 2009; 8: 108.
7. **Chaput N, De Botton S, Obeid M, et al.** Molecular determinants of immunogenic cell death: surface exposure of calreticulin makes the difference. *J Mol Med.* 2007; 85: 1069-76.
8. **Apetoh L, Mignot G, Panaretakis T, et al.** Immunogenicity of anthracyclines: moving towards more personalized medicine. *Trends Mol Med.* 2008; 14: 141-51.
9. **Obeid M, Testiere A, Ghiringhelli F, et al.** Calreticulin exposure dictates the immunogenicity of cancer cell death. *Nat Med.* 2007; 13: 54-61.
10. **Obeid M, Tesniere A, Panaretakis T, et al.** Ecto-calreticulin in immunogenic chemotherapy. *Immunol Rev.* 2007; 220: 22-34.
11. **Ghigo D, Riganti C, Gazzano E, et al.** Cycling of NADPH by glucose 6-phosphate dehydrogenase optimizes the spectrophotometric assay of nitric oxide synthase activity in cell lysates. *Nitric Oxide* 2006; 15: 148-53.
12. **Brusa D, Garetto S, Chiorino G, et al.** Post-apoptotic tumors are more palatable to dendritic cells and enhance their antigen cross-presentation activity. *Vaccine* 2008; 26: 6422-32.
13. **Wojciak-Stothard B, Torondel B, Zhao L, et al.** Modulation of Rac1 activity by ADMA/DDAH regulates pulmonary endothelial barrier function. *Mol Biol Cell.* 2009; 20: 33-42.
14. **Chen H, Levine YC, Golan DE, et al.** Atrial natriuretic peptide-initiated cGMP pathways regulate vasodilator-stimulated phosphoprotein phosphorylation and angiogenesis in vascular endothelium. *J Biol Chem.* 2008; 283: 4439-47.
15. **Pratesi G, Petrangolini G, Tortoreto M, et al.** Therapeutic synergism of gemcitabine and CpG-oligodeoxynucleotides in an orthotopic human pancreatic carcinoma xenograft. *Cancer Res.* 2005; 65: 6388-93.

16. **Braly P, Nicodemus CF, Chu C, et al.** The immune adjuvant properties of front-line carboplatin-paclitaxel: a randomized phase 2 study of alternative schedules of intravenous oregovomab chemoimmunotherapy in advanced ovarian cancer. *J Immunother.* 2009; 32: 54-65.
17. **Stoychkov JN, Schultz RM, Chirigos MA, et al.** Effects of adriamycin and cyclophosphamide treatment on induction of macrophage cytotoxic function in mice. *Cancer Res.* 1979; 39: 3014-17.
18. **Ho RL, Maccubbin D, Zaleskis G, et al.** Development of a safe and effective adriamycin plus interleukin 2 therapy against both adriamycin-sensitive and -resistant lymphomas. *Oncol Res.* 1993; 5: 373-81.
19. **Weigert A, Brüne B.** Nitric oxide, apoptosis and macrophage polarization during tumor progression. *Nitric Oxide* 2008; 19: 95-102.
20. **Banerjea A, Ahmed S, Hands RE, et al.** Colorectal cancers with microsatellite instability display mRNA expression signatures characteristic of increased immunogenicity. *Mol Cancer* 2004; 3: 21-32.
21. **Tufi R, Panaretakis T, Bianchi K, et al.** Reduction of endoplasmic reticulum Ca²⁺ levels favors plasma membrane surface exposure of calreticulin. *Cell Death Differ.* 2008; 15: 274-82.
22. **Oyadomari S, Takeda K, Takiguchi M, et al.** Nitric oxide-induced apoptosis in pancreatic b cells is mediated by the endoplasmic reticulum stress pathway. *Proc Nat Acad Sci.* 2001; 98:10845-50.
23. **Panaretakis T, Joza N, Modjtahedi N, et al.** The co-translocation of ERp57 and calreticulin determines the immunogenicity of cell death. *Cell Death Differ.* 2008; 15: 1499-1509.
24. **Molinari A, Calcabrini A, Meschini S, et al.** Subcellular detection and localization of the drug transporter P-glycoprotein in cultured tumor cells. *Curr Protein Pept Sci.* 2002; 3: 653-70.
25. **Van Duyn Graham L, Sweetwyne MT, Pallero MA, Murphy-Ullrich JE.** Intracellular Calreticulin Regulates Multiple Steps in Fibrillar Collagen Expression, Trafficking, and Processing into the Extracellular Matrix. *J Biol Chem.* 2010; 285: 7067-78.
26. **MacDiarmid JA, Amaro-Mugridge NB, Madrid-Weiss J, et al.** Sequential treatment of drug-resistant tumors with targeted minicells containing siRNA or a cytotoxic drug. *Nat Biotech.* 2009; 27: 643-54.

Figures

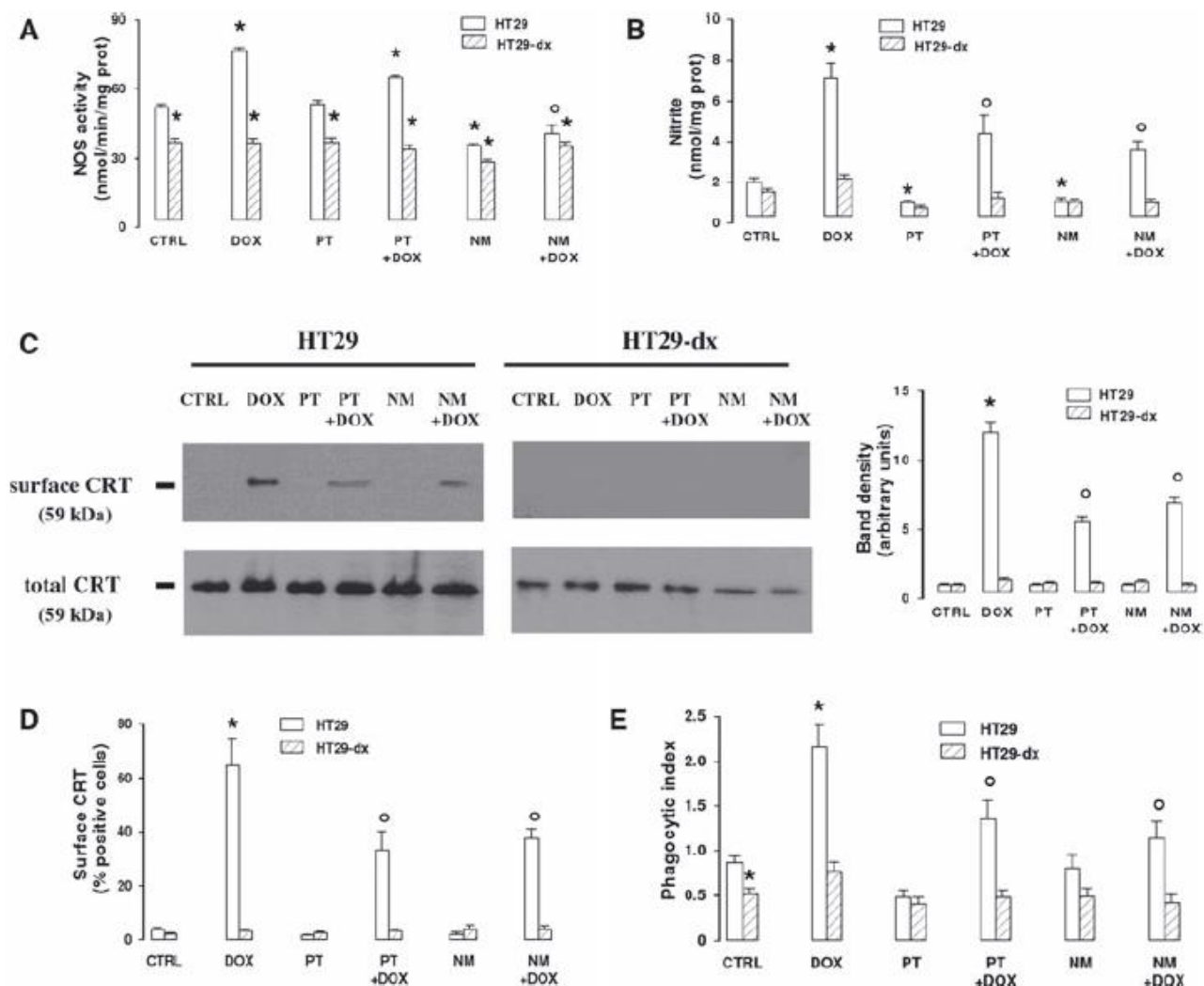


Figure 1. Effects of PTIO and L-NMMA on doxorubicin-induced NO synthesis, CRT translocation and tumour cells phagocytosis.

HT29 and HT29-dx cells were cultured for 6 h in the absence (*CTRL*) or in the presence of doxorubicin (5 μ mol/L, *DOX*), alone or together with the NO scavenger PTIO (100 μ mol/L, *PT*) or the NOS inhibitor L-NMMA (1 mmol/L, *NM*). Then the following assays were performed. (A) The NOS activity was measured in the cell lysates by a spectrophotometric

assay. Measurements were performed in triplicate. Data are presented as means \pm SE (n = 3). Vs CTRL HT29: * $p < 0.01$; vs DOX: ° $p < 0.001$. **(B)** Colorimetric detection of nitrite amounts in cell culture medium was performed in duplicate. Data are presented as means \pm SE (n = 4). Vs CTRL HT29: * $p < 0.001$; vs DOX: ° $p < 0.05$. **(C)** Western blot analysis of biotinylated surface CRT and of total CRT was performed as reported under Methods. The figure is representative of three experiments with similar results. The band density ratio between surface and total CRT was expressed as arbitrary units. Vs CTRL HT29: * $p < 0.001$; vs DOX: ° $p < 0.01$. **(D)** Flow cytometry analysis of cells positive for surface CRT was performed in duplicate as described in the Methods section. Data are presented as means \pm SE (n = 3). Vs CTRL HT29: * $p < 0.001$; vs DOX: ° $p < 0.02$. **(E)** The phagocytosis of HT29 and HT29-dx cells by iDCs was measured in duplicate by flow cytometry (see Methods section for details). Data are presented as means \pm SE (n = 3). Vs CTRL HT29: * $p < 0.05$; vs DOX: ° $p < 0.05$.

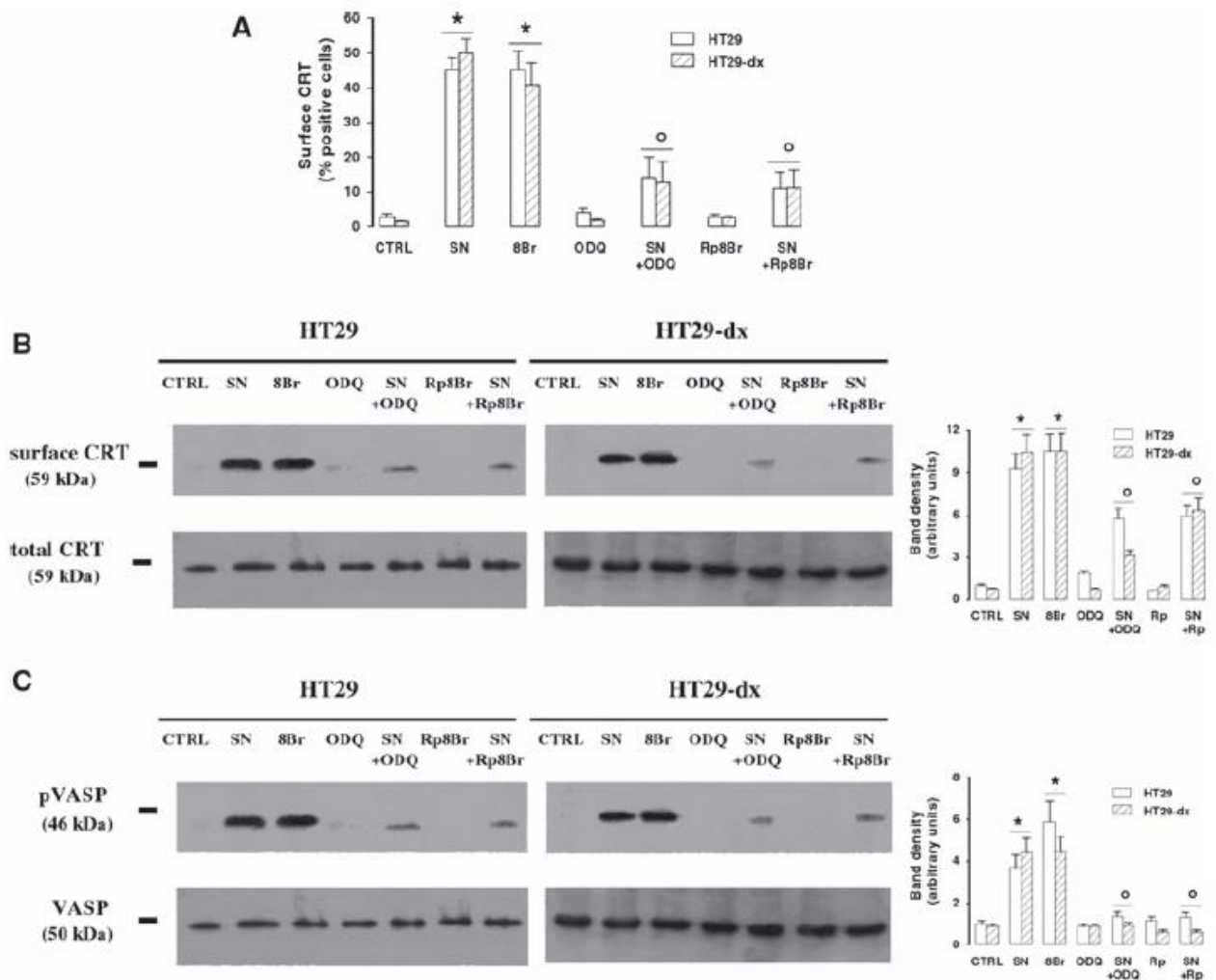


Figure 2. Effect of NO/cGMP pathway on CRT translocation.

HT29 and HT29-dx cells were treated for 1 h with fresh medium (*CTRL*), SNAP (100 $\mu\text{mol/L}$, *SN*), 8-Br-cGMP (10 $\mu\text{mol/L}$, *8Br*), ODQ (10 $\mu\text{mol/L}$, *ODQ*) and Rp-8-Br-cGMPs (10 $\mu\text{mol/L}$, *Rp8Br*), in different combinations, then subjected to the following investigations.

(A) The percentage of cells positive for surface CRT was measured in duplicate by FACS analysis as described in the Methods section. Data are presented as means \pm SE ($n = 3$). Vs CTRL HT29: * $p < 0.001$; vs SN: $^{\circ} p < 0.002$. (B) Biotinylated surface CRT and total CRT were measured in Western blotting experiments, as reported in the Methods section. The figure is representative of three experiments with similar results. The band density ratio

between surface and total CRT was expressed as arbitrary units. Vs CTRL HT29: * $p < 0.001$; vs SN: ° $p < 0.02$. (C) Western blot analysis of VASP and phospho(Ser239)-VASP was performed on cytosolic extracts as described under Methods. The figure is representative of three experiments with similar results. The the band density ratio between phospho(Ser239)-VASP and total VASP was expressed as arbitrary units. Vs CTRL HT29: * $p < 0.01$; vs SN: ° $p < 0.02$.

HT29 and HT29-dx cells were treated for 1 h with fresh medium (*CTRL*), SNAP (100 $\mu\text{mol/L}$, *SN*), 8-Br-cGMP (10 $\mu\text{mol/L}$, *8Br*), latrunculin A (200 nmol/L, *LA*), in different combinations, then the following experiments were performed. **(A)** The percentage of cells positive for surface CRT, obtained by FACS analysis, was calculated in duplicate as described in the Methods section. Data are presented as means \pm SE ($n = 3$). Vs CTRL HT29: * $p < 0.02$ vs SN: $^{\circ} p < 0.02$. **(B)** Biotinylated surface CRT and total CRT were measured by Western blot analysis as reported in the Methods section. The figure is representative of three experiments with similar results. The band density ratio between surface CRT and total CRT was expressed as arbitrary units. Vs CTRL HT29: * $p < 0.001$; vs SN: $^{\circ} p < 0.01$. **(C)** Cells were stained with phalloidin-tetramethylrhodamine B isothiocyanate to visualize actin fibres; surface CRT was detected by an anti-CRT antibody, as specified in the Methods section. The micrographs are representative of three experiments with similar results.

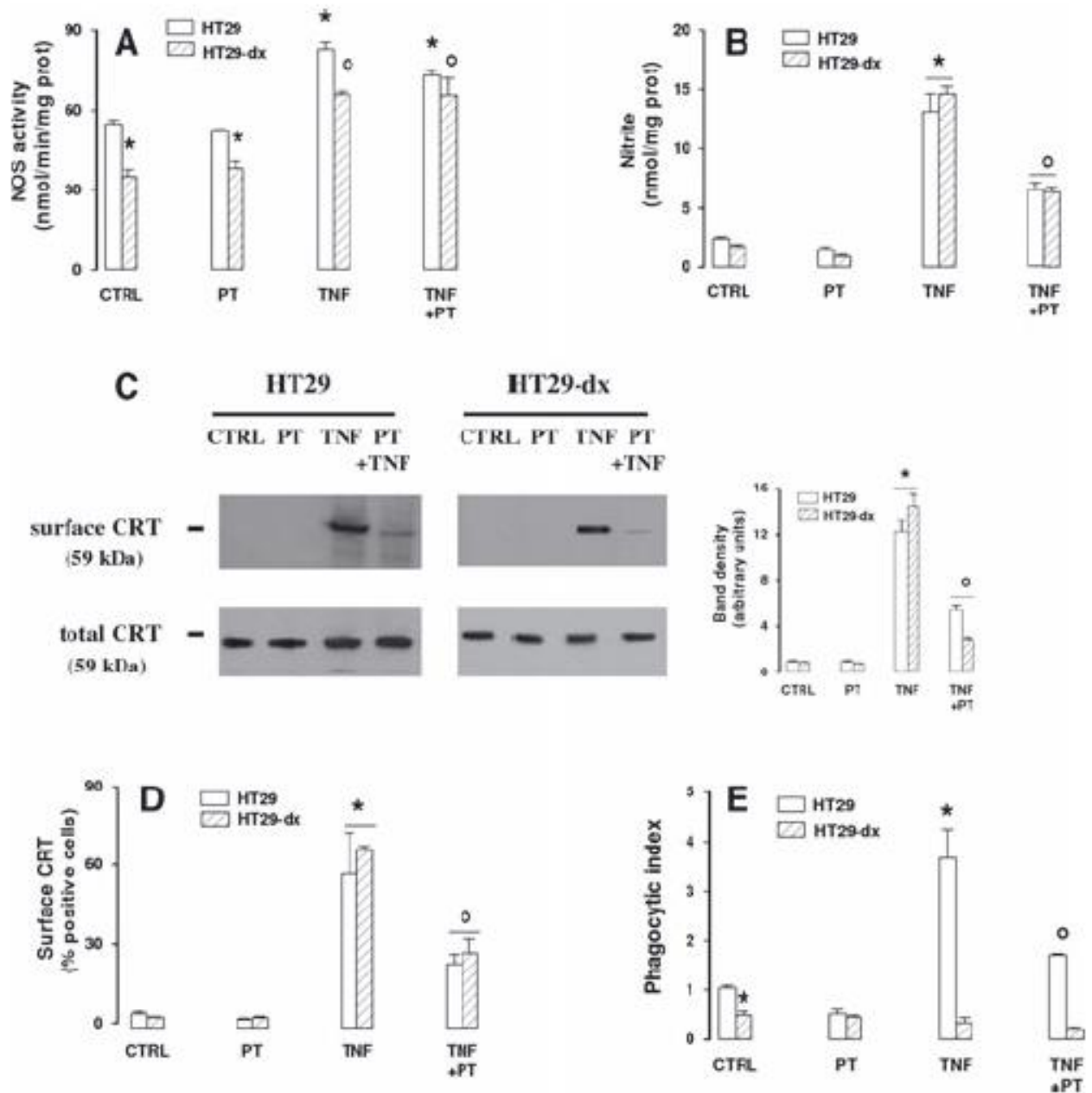


Figure 4. Effects of TNF- α on doxorubicin-induced NO synthesis, CRT translocation and tumour cells phagocytosis.

HT29 and HT29-dx cells were cultured for 6 h in the absence (*CTRL*) or presence of the iNOS inducer TNF- α (50 ng/mL, *TNF*), alone or together with the NO scavenger PTIO (100 μ mol/L, *PT*), then cells were subjected to the following investigations. (A)

Spectrophotometric detection of the NOS activity in cell lysates. Measurements were performed in triplicate. Data are presented as means \pm SE (n = 3). Vs CTRL HT29: * $p < 0.001$; vs CTRL HT29-dx: ° $p < 0.005$. **(B)** The nitrite levels in the culture supernatant, assessed by Griess method, were measured in duplicate. Data are presented as means \pm SE (n = 4). Vs CTRL HT29: * $p < 0.01$; vs TNF: ° $p < 0.005$. **(C)** Biotinylated surface CRT and total cell CRT expression was measured by Western blot experiments, as reported under Methods. The figure is representative of three experiments with similar results. The band density ratio between surface and total CRT was expressed as arbitrary units. Vs CTRL HT29: * $p < 0.01$; vs TNF: ° $p < 0.005$. **(D)** The percentage of cells positive for surface CRT was performed in duplicate by FACS analysis as described in the Methods section. Data are presented as means \pm SE (n = 3). Vs CTRL HT29: * $p < 0.05$; vs TNF: ° $p < 0.05$. **(E)** The rate of HT29 and HT29-dx cells phagocytized by iDCs was measured in duplicate by flow cytometry (see Methods section for details). Data are presented as means \pm SE (n = 3). Vs CTRL HT29: * $p < 0.05$; vs TNF: ° $p < 0.05$.

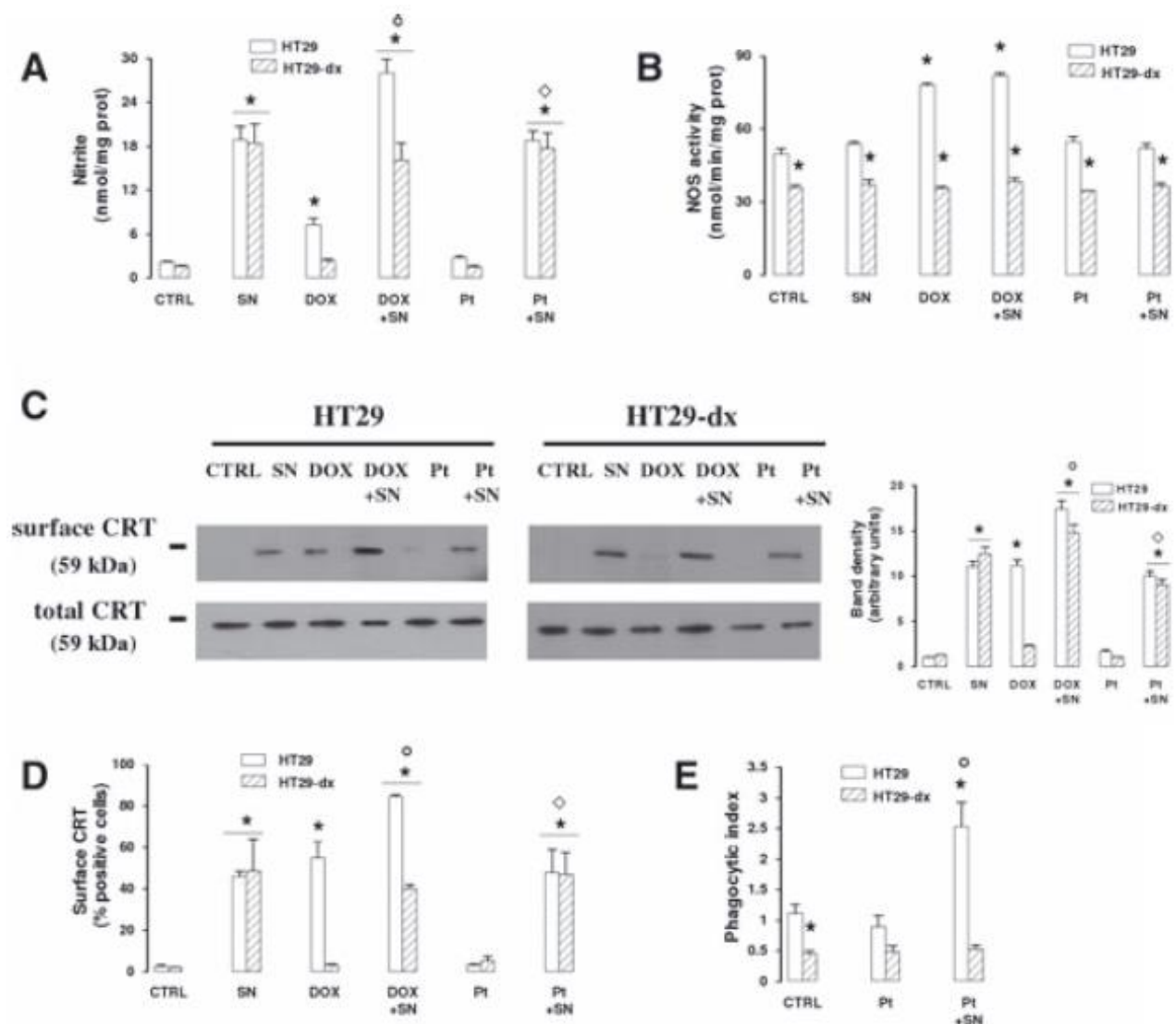


Figure 5. Effect of SNAP and anticancer drugs on CRT translocation and phagocytosis in HT29 and HT29-dx cells.

HT29 and HT29-dx cells were incubated for 6 h in the absence (*CTRL*) or presence of the NO donor SNAP (100 μ mol/L, *SN*), doxorubicin (5 μ mol/L, *DOX*) or cisplatin (10 μ mol/L, *Pt*), in different combinations. Then the following investigations were performed. (A) The nitrite amount was detected in the supernatant of cell cultures in duplicate, as described in the Methods section. Data are presented as means \pm SE (n = 4). Vs CTRL HT29: * p < 0.005; vs DOX: ° p < 0.001; vs Pt: ◇ p < 0.001. (B) The NOS activity was measured

spectrophotometrically in the cell lysates. Measurements were performed in triplicate. Data are presented as means \pm SE (n = 3). Vs CTRL HT29: * $p < 0.005$. (C) Western blot analysis of biotinylated surface CRT and of total cell CRT was performed as reported under Methods. The figure is representative of three experiments with similar results. The band density ratio between surface and total CRT was expressed as arbitrary units. Vs CTRL HT29: * $p < 0.001$; vs DOX: $^{\circ} p < 0.002$; vs Pt: $^{\diamond} p < 0.02$. (D) The surface expression of CRT was assessed by flow cytometry analysis (see Methods section for details). Data are presented as means \pm SE (n = 4). Vs CTRL HT29: * $p < 0.001$; vs DOX: $^{\circ} p < 0.01$; vs Pt: $^{\diamond} p < 0.02$. (E) The uptake of HT29 and HT29-dx cells by iDCs was evaluated in duplicate by flow cytometry, as reported in the Methods section. Data are presented as means \pm SE (n = 3). Vs CTRL HT29: * $p < 0.01$; vs Pt: $^{\circ} p < 0.02$.

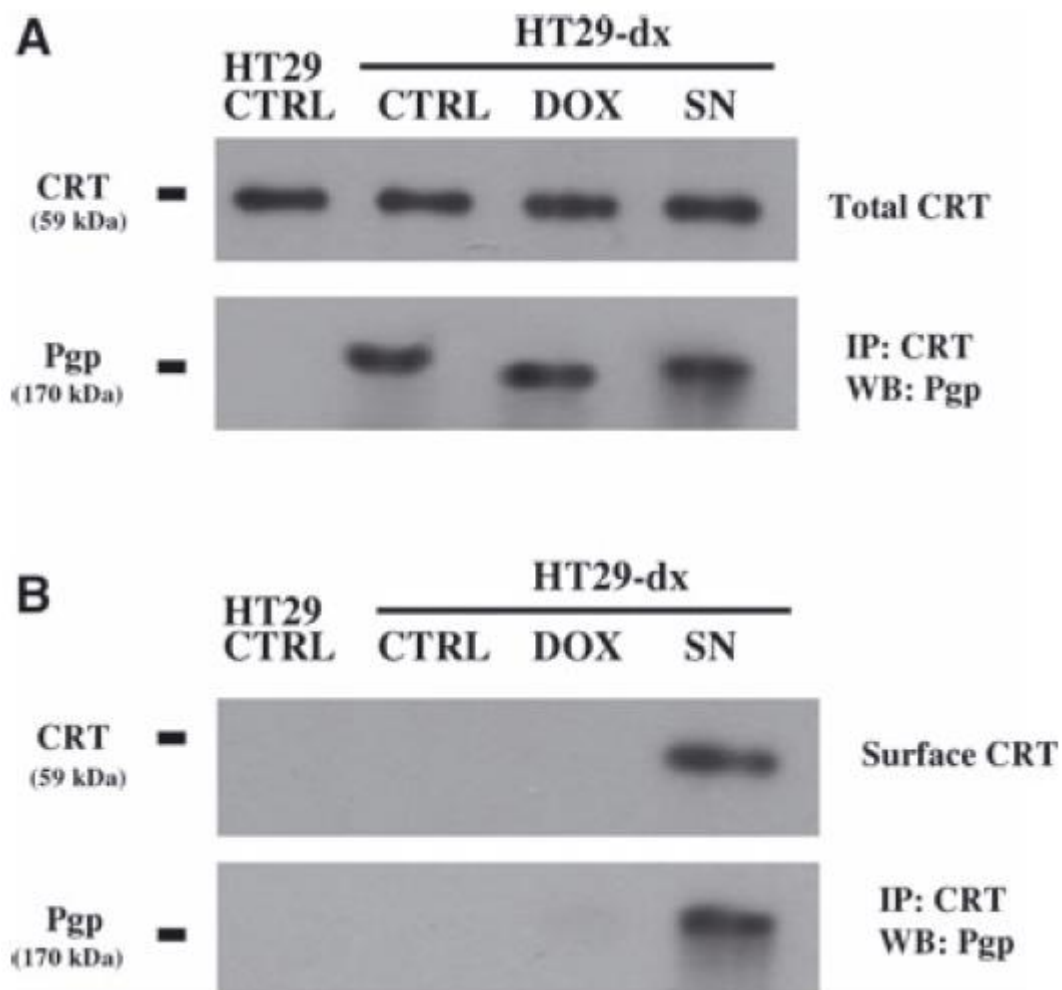


Figure 6. Co-immunoprecipitation of calreticulin and Pgp in HT29 and HT29-dx cells.

Cells were incubated for 6 h in the absence (*CTRL*) or presence of doxorubicin (5 $\mu\text{mol/L}$, *DOX*) or SNAP (100 $\mu\text{mol/L}$, *SN*), then they were lysed and subjected to ultracentrifugation to isolate the ER-enriched fraction (panel **A**). In parallel, in an aliquot of cells incubated under the same experimental conditions, the surface proteins were isolated by a biotinylation assay (panel **B**). Each sample was immunoprecipitated (*IP*) with an anti-CRT antibody and probed with an anti-Pgp or an anti-CRT antibody by Western blotting (*WB*), as reported in the Methods section. The results shown here are representative of two similar experiments, giving superimposable results.

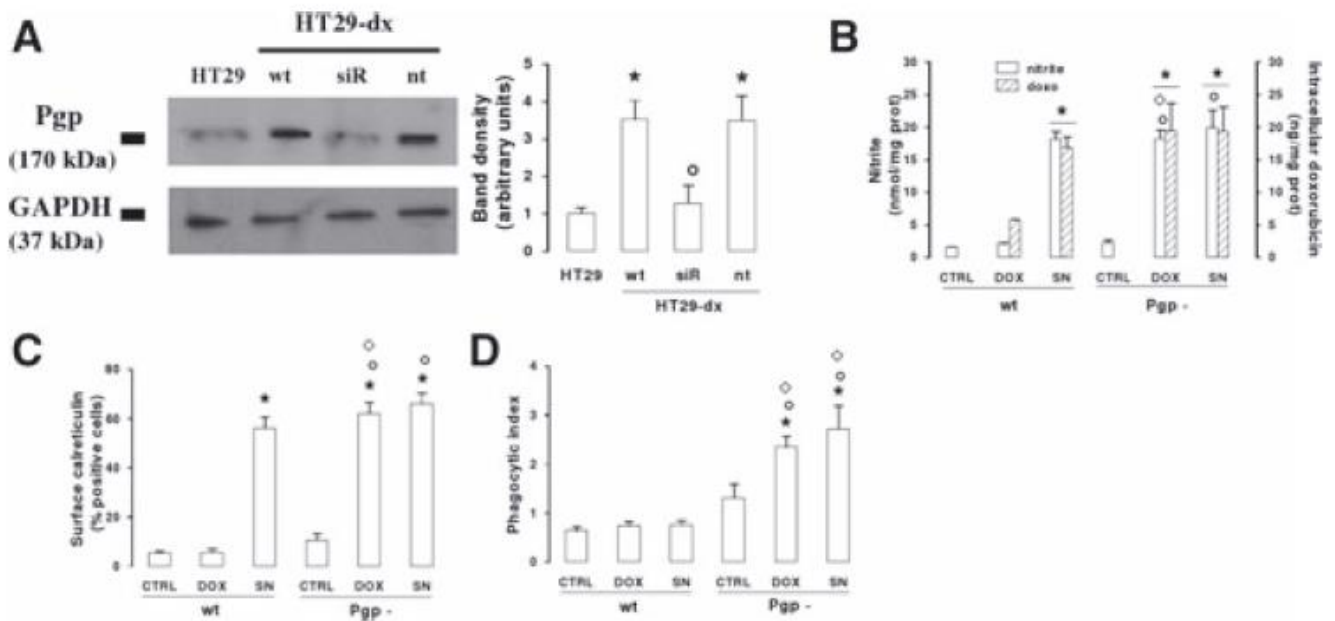


Figure 7. Effect of Pgp knocking-down on CRT exposure and HT29-dx cell phagocytosis.

Non-silenced HT29-dx cells (*wt*) or HT29-dx cells silenced for Pgp (*Pgp-*) were incubated for 6 h with fresh medium (*CTRL*), doxorubicin (5 μ mol/L, *DOX*) or SNAP (100 μ mol/L, *SN*), then subjected to the following investigations. (**A**) Western blot detection of Pgp. HT29-dx cells were grown for 72 h in the absence (*wt*) or presence of siRNA sequences (*siR*) targeting Pgp gene, as reported in the Methods section. When indicated, a non-targeting scrambled siRNA sequence (*nt*) was added instead of siRNA for Pgp. The expression of Pgp was detected by Western blot analysis, comparing HT29-dx with untreated HT29 cells. The expression of the housekeeping protein GAPDH was measured as equal control loading. The the band density ratio between Pgp and GAPDH was expressed as arbitrary units. Vs HT29: * $p < 0.05$; vs HT29-dx wt: $^{\circ} p < 0.05$. (**B**) The nitrite synthesis in the culture supernatant (*open bars*) and the intracellular doxorubicin accumulation (*hatched bars*) were measured in duplicate, as described in the Methods section. Data are presented as means \pm SE ($n = 4$). For

nitrite: vs CTRL wt: * $p < 0.05$; vs CTRL Pgp-: ° $p < 0.05$; vs DOX wt: ◇ $p < 0.01$. For doxorubicin: vs DOX wt: * $p < 0.05$. **(C)** The surface expression of CRT, assessed by flow cytometry analysis as reported under Methods, was measured in duplicate. Data are presented as means \pm SE (n = 4). Vs CTRL wt: * $p < 0.01$; vs CTRL Pgp-: ° $p < 0.01$; vs DOX wt: ◇ $p < 0.002$. **(D)** The phagocytosis rate of HT29-dx cells by iDCs was evaluated in duplicate by flow cytometry (see Methods section). Data are presented as means \pm SE (n = 3). Vs CTRL wt: * $p < 0.05$; vs CTRL Pgp-: ° $p < 0.05$; vs DOX or SN wt respectively: ◇ $p < 0.02$.

Supplementary Figure

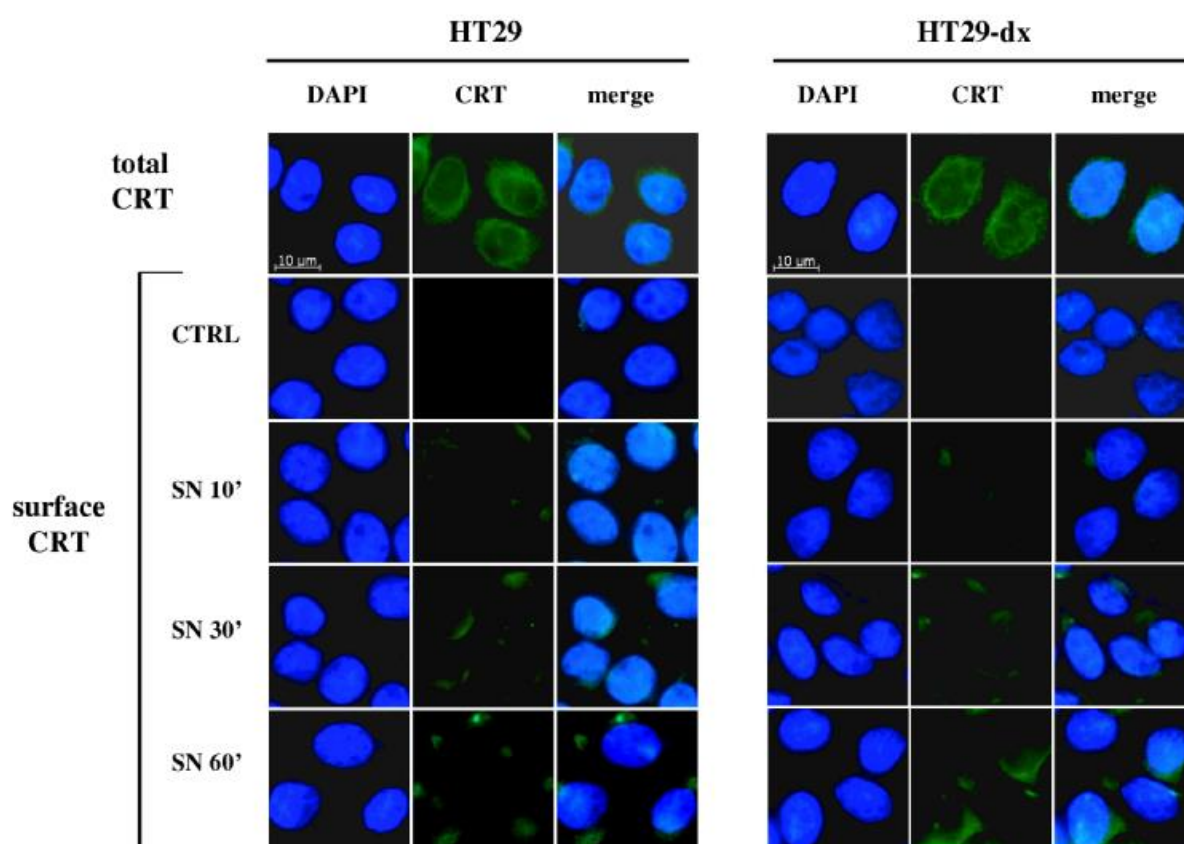


Figure S1. Kinetics of CRT translocation on cell surface elicited by NO.

HT29 and HT29-dx cells were treated for 1 h with fresh medium (*CTRL*) or SNAP (100 μmol/L for 10, 30 and 60 minutes, *SN*), then washed and stained for CRT. Total CRT was detected in untreated cells after fixation and permeabilization; CRT present on cell surface was evaluated in non-permeabilized cells. The micrographs are representative of three experiments with similar results.